Catal. Today, submitted

Simultaneous abatement of NO and N_2O with CH_4 over modified Al_2O_3 supported Pt,Pd,Rh

Maria Cristina Campa[a,*], Aidan M. Doyle[b], Giuseppe Fierro[a], Daniela Pietrogiacomi[c]

[a] *CNR-Istituto per lo Studio dei Materiali Nanostrutturati, c/o Department of Chemistry, "Sapienza" University of Rome, P.le Aldo Moro, 5 – 00185 Roma, Italy*

[b] *Department of Natural Sciences, Manchester Metropolitan University, Chester St, Manchester, M1 5GD, United Kingdom*

[c] *Department of Chemistry, "Sapienza" University of Rome, P.le Aldo Moro, 5 – 00185 Roma, Italy*

*Corresponding author:

Dr. Maria Cristina Campa

CNR-Istituto per lo Studio dei Materiali Nanostrutturati,

c/o Department of Chemistry, "Sapienza" University of Rome, P.le Aldo Moro, 5

00185 Roma, Italy.

Fax: +39-06-49913175

E-mail address: mariacristina.campa@cnr.it

Abstract

Pt, Pd and Rh supported on Al_2O_3-SiO_2 and Al_2O_3-ZrO_2, prepared by adsorbing noble metal ions from salt aqueous solutions on well-mixed supports, were characterized by XRD, N_2 physisorption and FESEM, and studied for the simultaneous abatement of NO and N_2O by selective catalytic reduction in the presence of O_2 using CH_4 as reductant (SCR_{sim}). To give a better insight into the simultaneous process, the reactions related to SCR_{sim} (SCR_{NO}, SCR_{N2O}, CH_4 combustion), as well as the abatements in the absence of O_2 (CR_{sim}, CR_{NO}, CR_{N2O}), and the N_2O decomposition by itself and in the presence of O_2 and NO, were investigated. The catalytic measurements were performed in a flow apparatus with GC analysis of reactants and products.

Catalytic results showed that Pt,Pd,Rh/Al_2O_3-SiO_2 and Pt,Pd,Rh/Al_2O_3-ZrO_2 are effective catalysts for SCR_{sim} above 400 °C from feeds containing O_2/CH_4 less than 1, yielding complete NO and N_2O conversions and complete selectivity to CO_2 and N_2. At lower temperatures, N_2O and NO are unconverted and only the competitive CH_4 combustion occurs. Compared to the separate NO and N_2O abatement reactions, a slight shift in activity towards higher temperatures occurs in SCR_{sim}. Such a shift can be related to the possible formation of strongly adsorbed NO_y-like species formed in the presence of NO and competing with the N_2O adsorption sites. The poisoning effect of these species disappears above a threshold-like temperature (about 300 °C), suggesting that above this temperature the high surface-O mobility, guaranteeing a partial reduction of the noble metal ions by CH_4, sustains the reductive reactions of both NO and N_2O.

Keywords: NO_x and N_2O simultaneous abatement with CH_4; Pt,Pd,Rh supported on Al_2O_3-SiO_2 or Al_2O_3-ZrO_2; SCR reactions; N_2O decomposition

1. Introduction

Nitrogen oxides are formed in nitric acid and adipic acid production, fossil fuel power plants and by the thermal oxidation of atmospheric nitrogen in internal combustion engines. The main problem with nitric oxide, NO, is its toxicity especially in populated areas, while nitrous oxide, N_2O, is a particularly potent greenhouse gas [1]. Efforts have been made to control these emissions by imposing legislation that limits the levels permitted. Since it is not possible to prevent nitrogen oxides formation sufficiently to meet legislative limits, after-treatment systems using heterogeneous catalysts have been successfully devoted to their abatement [2-5]. These catalysts operate by decomposing NO_x directly to N_2 and O_2 or reducing NO_x with e.g. NH_3, H_2, CO or CH_4 to form predominantly N_2, H_2O and CO_2 [2,6-8]. CH_4 is a promising reducing agent for deNO_x reactions due to a cheap and plentiful supply of natural gas (predominantly CH_4) as a result of shale bed fracking. Furthermore, CH_4 has the highest H:C ratio (4:1) of any hydrocarbon so is increasingly being used as a low carbon substitute for diesel in dual fuel engines for heavy good vehicles (HGVs) as a plausible first step towards decarbonization of the transportation sector [9].

Noble metal based catalysts continue to be an important class of materials devoted to deNO_x. Pt, Pd and Rh are the most used precious metals in Three-Way-Converter (TWC) catalysts to decrease the exhaust gas emissions from engines [10,11,12]. In particular, Pt and Pd are used for the oxidative component of three-way catalysis, while Rh is necessary for good NO_x removal capabilities [12]. A synergism among Pd and Pt for oxidation of hydrocarbons (HCs) and carbon monoxide was also found for different systems [13].

The bulk of the research effort has been given to the abatement of NO and NO_2, with less attention on N_2O [14,15]. This is despite the formation of N_2O as a by-product depending on the engine operating conditions (air-to-fuel ratio, operation temperature), catalyst composition and the presence of deactivating molecules such as H_2O and SO_2 in the exhaust stream. It is therefore interesting for practical applications to find a catalyst for the simultaneous abatement of NO and N_2O.

While there are many laboratory studies describing the abatement of either NO or N_2O, i.e. in separate experiments, there are relatively few reports of catalysts that remove both pollutants simultaneously. NO and N_2O were reduced sequentially in dual-bed reactors over (first) Co-ZSM-5 and (second) Pd/Fe-ZSM-5 using C_3H_8 as reductant [16], In/Al_2O_3 and Ru/Al_2O_3 using C_3H_8 [17] and over Pd-modified perovskites using H_2 for NO and decomposition for N_2O [18]. Simultaneous catalytic abatement of NO and N_2O was studied

over Ag/ZSM-5 [19] and zeolite supported Fe catalysts using NH_3 [20-23], and various hydrocarbons [24,25]. The industrial EnviNOx® process [26] performs the abatement of NO_x and N_2O over iron-containing zeolite catalysts in two catalytic beds, where NO_x is abated by NH_3 and N_2O by hydrocarbons or *via* decomposition assisted by NO [27,28].We recently reported the simultaneous abatement of NO and N_2O in the presence of O_2 with C_3H_6 over CoO_x and FeO_x supported on ZrO_2 [29], and with CH_4 over Fe-, Co- and Ni-exchanged MOR [30]. In a separate study using *operando* FTIR we proposed a reaction pathway for the selective catalytic reduction of NO and N_2O with CH_4 over Fe-, Co- and Ni-MOR catalysts [31].

In this paper, we explore the simultaneous abatement of NO and N_2O over platinum group metal catalysts, Pt, Pd and Rh, (more similar to those in 'realistic' TWCs) supported on Al_2O_3-SiO_2 and Al_2O_3-ZrO_2, through the selective catalytic reduction in the presence of O_2 using CH_4 as reductant (SCR_{sim}). Our choice was motivated by the fact that, besides being a promoter of NO activation, Rh (in supported systems, in modified zeolites, in hydrotalcite derived metal oxides and in bimetallic systems) is the most active noble metal for the N_2O decomposition (deN_2O) [15], this making Rh an attractive component of a catalyst for the simultaneous abatement of NO and N_2O. The activity and selectivity of these catalysts were also evaluated at different O_2 content in the feed as the SCR efficiency is strongly depending if lean or rich conditions of feeding mixture are used [32]. Moreover, in order to shed more light on the SCR_{sim}, the SCR with the single reactant (SCR_{NO}, SCR_{N2O}), as well as the catalytic reductions in the absence of O_2 (CR_{sim}, CR_{NO}, CR_{N2O}), were investigated. Studies are also included of the N_2O decomposition by itself and in the presence of O_2 and NO, and the CH_4 combustion reaction.

2. Experimental

2.1. Materials

55.2 mg of Rh(II)acetate (Alfa, 98%), 46 mg of $Pd(NO_3)_2$ (Alfa, 99.8%) and 42 mg of $PtCl_4$ (Alfa, 99.9%) were placed in separate 25 cm^3 volumetric flasks. 5 cm^3 of approximately 30% aqueous NH_4OH (Honeywell) was added to the flask containing Rh, and each flask was filled with deionized water, subjected to ultrasonic treatment for 30 minutes, then made up to the mark with deionized water. All three solutions were added to 2.0 g of equal masses of well-mixed supports γ-Al_2O_3, amorphous aluminosilica containing >95% silica so referred to

here as SiO_2, and monoclinic ZrO_2 to give catalysts Pt,Pd,Rh/Al_2O_3-SiO_2 and Pt,Pd,Rh/Al_2O_3-ZrO_2. The resulting suspension was subjected to ultrasonic treatment for 45 minutes, stirred overnight, filtered, washed with deionized water, dried and calcined for 4 h in air at 550 °C.

2.2. Characterization

A Rigaku NEX-CG XRF spectrometer was used for elemental analysis using the loose powder method under vacuum. The Pt, Pd, and Rh wt%, as measured by XRF, are reported in Table 1.

X-Ray Diffraction (XRD) patterns were obtained with a Philips PW 1729 diffractometer using Cu Kα (Ni-filtered) radiation (λ = 1.5406 Å) in the 10-70° 2θ range (step size 0.02°; step time 1.25 s) and an X-ray tube operated at 40 kV and 20 mA.

Nitrogen adsorption/desorption measurements were carried out using a Micromeritics ASAP 2020 surface area analyzer at -196 °C. Samples were degassed under vacuum ($p < 10^{-3}$ Pa) for 12 h at 300 °C prior to analysis. BET surface areas of the samples were calculated in the relative pressure range 0.05-0.30.

The catalyst's morphology as fresh sample and after reaction was investigated by Field-Emission Scanning Electron Microscopy (FESEM) using an AURIGA Zeiss 405 HR-FESEM instrument equipped with an Energy Dispersive X-ray Spectroscopy (EDXS) Bruker apparatus for elemental detection.

2.3. Catalytic experiments

The catalytic activity was measured in a flow apparatus at atmospheric pressure in steady state conditions. The apparatus included an inlet gas section for feeding five gas flows (He, 3% NO in He, 3% N_2O in He, 1.5% CH_4 in He, and 10% O_2 in He). The regulation of each gas flow was made independently by mass flow controller-meters (MKS Instruments). In order to make homogeneous the resulting stream, the five gases' flows were mixed in a glass ampoule before entering the reactor. Gas mixtures were purchased from RIVOIRA and used without further purification. The reactor was made of silica with an internal sintered frit of about 12 mm diameter supporting the powdered catalyst. Reactants and products were analysed by a gas-chromatograph (Agilent 7890A GC system) equipped with three columns (Molsieve 5A, for detecting O_2, N_2 and CO, Porapack Q for detecting CO_2 and N_2O, and Na_2SO_4-doped alumina for detecting CH_4) and two detectors (TCD and FID). The C-balance was calculated for all experiments, whereas the N-balance was calculated only for experiments in the absence of ($NO+O_2$) in the feed, NO_2 not being detectable by GC-analysis.

A portion of sample (0.250 g) was activated according to a standard procedure, i.e. by feeding 2.5% O_2/He mixture (100 cm^3 min^{-1}) from RT to 773 K and then maintaining isothermally at 773 K for 90 min. After this treatment, the reactor was bypassed and the temperature adjusted to the desired value. In a typical catalytic run the reaction temperature was changed at random without intermediate activation treatment. Catalysis was run by contacting the catalyst with feeds typically containing N_2O (4000 ppm), NO (4000 ppm), CH_4 (4000 ppm) and O_2 (20000, 5000, 2500 ppm) (v/v, He as balance), or purposely changed as indicated in the Figs. The total flow rate was maintained at 50 cm^3 STP/min, and space velocity (GHSV) was 12000 NL kg h^{-1}. Conversions obtained at various (sample weight)/(flow rate) ratios (W/F) indicated that, in our conditions, the reaction is under kinetic control without diffusion effect.

The N_2O, CH_4 or O_2 conversion was calculated from (molecules consumed)/(molecules injected):

$$N_2O\ Conversion\ (\%) = 100 \cdot \frac{N_2O_{inlet} - N_2O_{outlet}}{N_2O_{inlet}}$$

$$CH_4\ Conversion\ (\%) = 100 \cdot \frac{CH_{4\ inlet} - CH_{4\ outlet}}{CH_{4\ inlet}}$$

$$O_2\ Conversion\ (\%) = 100 \cdot \frac{O_{2\ inlet} - O_{2\ outlet}}{O_{2\ inlet}}.$$

The total NO conversion in experiments without oxygen (CR_{NO} and CR_{sim}) was calculated from:

$$NO\ Conversion\ (\%) = 100 \cdot \frac{(NO_{inlet} - NO_{outlet})}{NO_{inlet}}.$$

The NO conversion to N_2 (%) in the absence of N_2O as reactant (CR_{NO} and SCR_{NO}) was calculated from

$$NO\ Conversion\ to\ N_2\ (\%) = 100 \cdot 2 \cdot \frac{N_{2\ outlet}}{NO_{inlet}}$$

whereas for the simultaneous abatement (SCR_{sim}) was:

$$NO\ Conversion\ to\ N_2\ (\%) = 100 \cdot 2 \cdot \frac{(N_{2\ outlet} - N_2O_{consumed})}{NO_{inlet}}$$

where $N_2O_{consumed} = (N_2O_{inlet} - N_2O_{outlet})$.

The CO_2 selectivity with respect to CO was calculated as:

$$CO_2\ Selectivity\ (\%) = 100 \cdot \frac{CO_{2\ outlet}}{CO_{2\ outlet} + CO_{outlet}}$$

The C-balance was calculated as (total C atoms injected)/(total C atoms emitted).The N-balance was calculated as (total N atoms injected)/(total N atoms emitted). When NO and O_2 are simultaneously present in the mixture, N-balance cannot be calculated as undetectable NO_2 is also formed.

3. Results and discussion

3.1. Catalyst characterization

The Pt, Pd, and Rh wt%, as measured by XRF, are reported in Table 1. Nitrogen adsorption-desorption isotherms, Fig. 1, are of Type IV classification for each of Pt,Pd,Rh/Al_2O_3-SiO_2 and Pt,Pd,Rh/Al_2O_3-ZrO_2 consistent with the presence of mesopores. Micropore volumes were approximately zero. The volumes adsorbed are significantly higher for Pt,Pd,Rh/Al_2O_3-SiO_2 over the full relative pressure range due to its higher degree of porosity. Further confirmation of this is seen in the higher total pore volumes, V_{total}, and BET surface areas for Pt,Pd,Rh/Al_2O_3-SiO_2, 0.30 cm^3 g^{-1} and 200 m^2 g^{-1}, versus 0.19 cm^3 g^{-1} and 67.2 m^2 g^{-1} for Pt,Pd,Rh/Al_2O_3-ZrO_2 (see Table 1). The higher specific surface area and porosity of Al_2O_3-SiO_2 support are very likely responsible for the higher noble metal uptake in the Pt,Pd,Rh/Al_2O_3-SiO_2 final catalyst.

Table 1: Pt, Pd and Rh content and textural features of catalysts (surface areas and total pore volumes).

Sample	Pt		Pd		Rh		S_{BET} [a] (m^2 g^{-1})	V_{total} [b] (cm^3 g^{-1})
	wt%	N_{surf} [c] (at nm^{-2})	wt%	N_{surf} [c] (at nm^{-2})	wt%	N_{surf} [c] (at nm^{-2})		
Pt,Pd,Rh/Al_2O_3-SiO_2	0.90	0.14	0.97	0.27	1.23	0.36	200	0.30
Pt,Pd,Rh/Al_2O_3-ZrO_2	0.65	0.30	0.23	0.19	0.27	0.23	67.2	0.19

[a] S_{BET} = BET specific surface areas (m^2 g^{-1})
[b] V_{total} = Total pore volumes (cm^3 g^{-1})
[c] N_{surf} = Noble metal density at the catalyst surface (at nm^{-2})

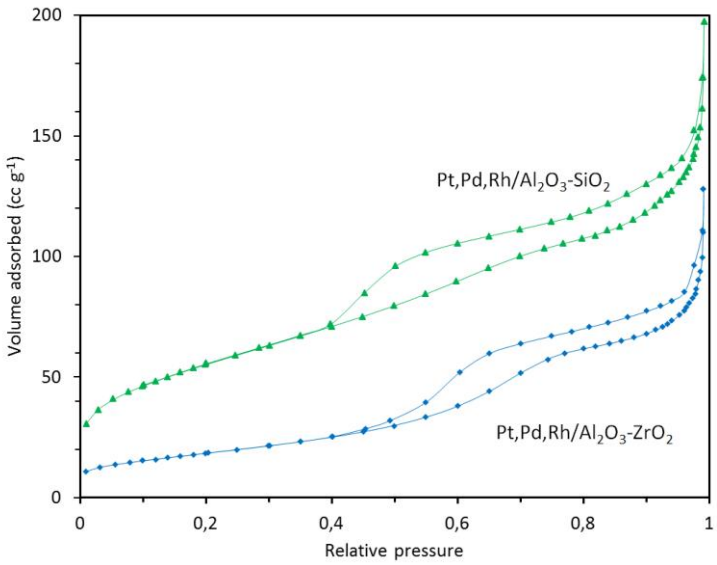

Figure 1. Nitrogen-adsorption-desorption isotherms of Pt,Pd,Rh/Al_2O_3-SiO_2 and Pt,Pd,Rh/Al_2O_3-ZrO_2.

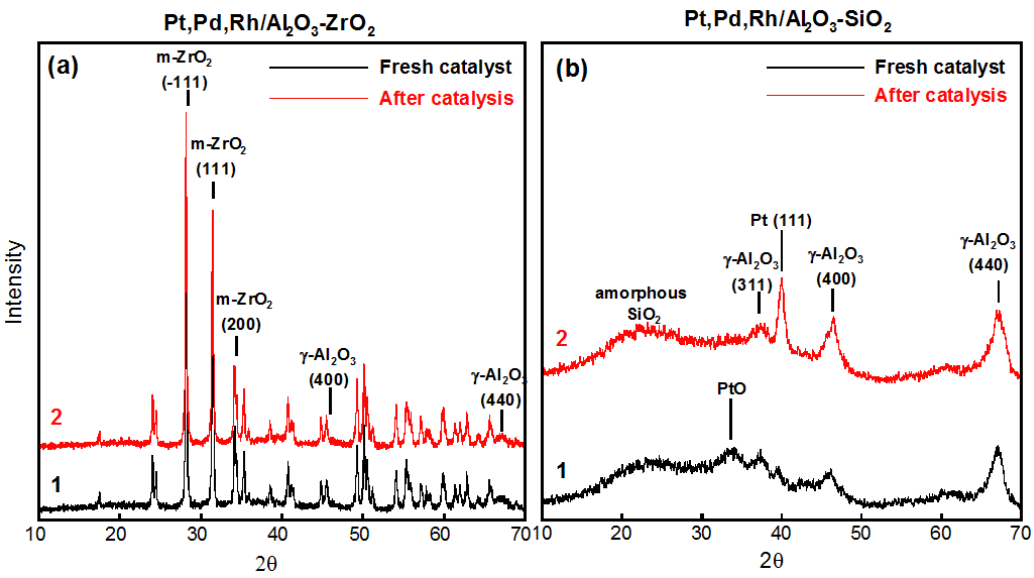

Figure 2. XRD patterns of (a) Pt,Pd,Rh/Al_2O_3-ZrO_2 and (b) Pt,Pd,Rh/Al_2O_3-SiO_2: fresh catalysts (patterns 1) and after catalysis (patterns 2). The vertical markers correspond to the most intense reflections of the monoclinic ZrO_2, γ-Al_2O_3, PtO and Pt reference compounds (see text for the JCPDS cards).

The XRD pattern of the fresh Pt,Pd,Rh/Al_2O_3-ZrO_2 catalyst (Fig. 2a, pattern 1) showed the most intense (400) and (440) reflections characteristic of the γ-Al_2O_3 crystallographic phase [JCPDS 10-425 card], and the reflections of monoclinic ZrO_2 (m-ZrO_2) [JCPDS card 37-1484]. The absence of XRD peaks for Pt, Pd and Rh, either as oxides or metals, on the fresh Pt,Pd,Rh/Al_2O_3-ZrO_2 catalyst suggests that the mean diameter of noble metal crystallites is below ca. 5 nm. After the catalytic runs, the XRD pattern of the Pt,Pd,Rh/Al_2O_3-ZrO_2 catalyst matched that of the fresh catalysts (Fig. 2a, pattern 2), suggesting that no remarkable structural changes occurred in the solid.

The XRD pattern of the fresh Pt,Pd,Rh/Al_2O_3-SiO_2 catalyst (Fig. 2b, pattern 1), besides the most intense reflections of γ-Al_2O_3, showed a diffuse peak of amorphous SiO_2 over the angular range 20° to 30° [33], and a small peak at about 33.5° corresponding to the most intense reflection of PtO [JCPDS card 43-1100]. After all the catalytic runs, the XRD pattern of Pt,Pd,Rh/Al_2O_3-SiO_2 catalyst showed the support reflections as in the fresh catalyst, but in addition a peak at about 40° corresponding to Pt metal [JCPDS cards 1-1194] appeared, indicating the PtO reduction occurred to some extent during catalysis. The mean size of Pt metal crystallites was about 10 nm maximum, as estimated by the Scherrer equation [34].

FESEM images of fresh Pt,Pd,Rh/Al_2O_3-ZrO_2 showed a few particles of Pt, Pd and Rh below 20 nm and many others with size well below 5 nm (Fig. 3a), in a number of locations, over ZrO_2 support. The corresponding EDX analysis showed that noble metals are uniformly spread on the imaged area, thus confirming a homogeneous dispersion (insets of Fig. 3a). If compared to fresh Pt,Pd,Rh/Al_2O_3-ZrO_2, the FESEM and EDX analyses on the catalyst after catalysis evidenced that the morphology was almost preserved after catalytic runs, as the noble metal particles remained unchanged both in size (up to ca. 20 nm) and distribution (Fig. 3b). A comparison of the Pt,Pd,Rh/Al_2O_3-ZrO_2 and Pt,Pd,Rh/Al_2O_3-SiO_2 catalysts after the catalytic runs (Fig. 3b and c) showed that the noble metals particle size and distribution are similar, this paralleling the rather close noble metals density at the catalyst surface (atoms/nm^2, see Table 1).

These results, as a whole, suggest that the noble metal particles were firmly anchored to the support, and did not undergo sintering under catalytic conditions.

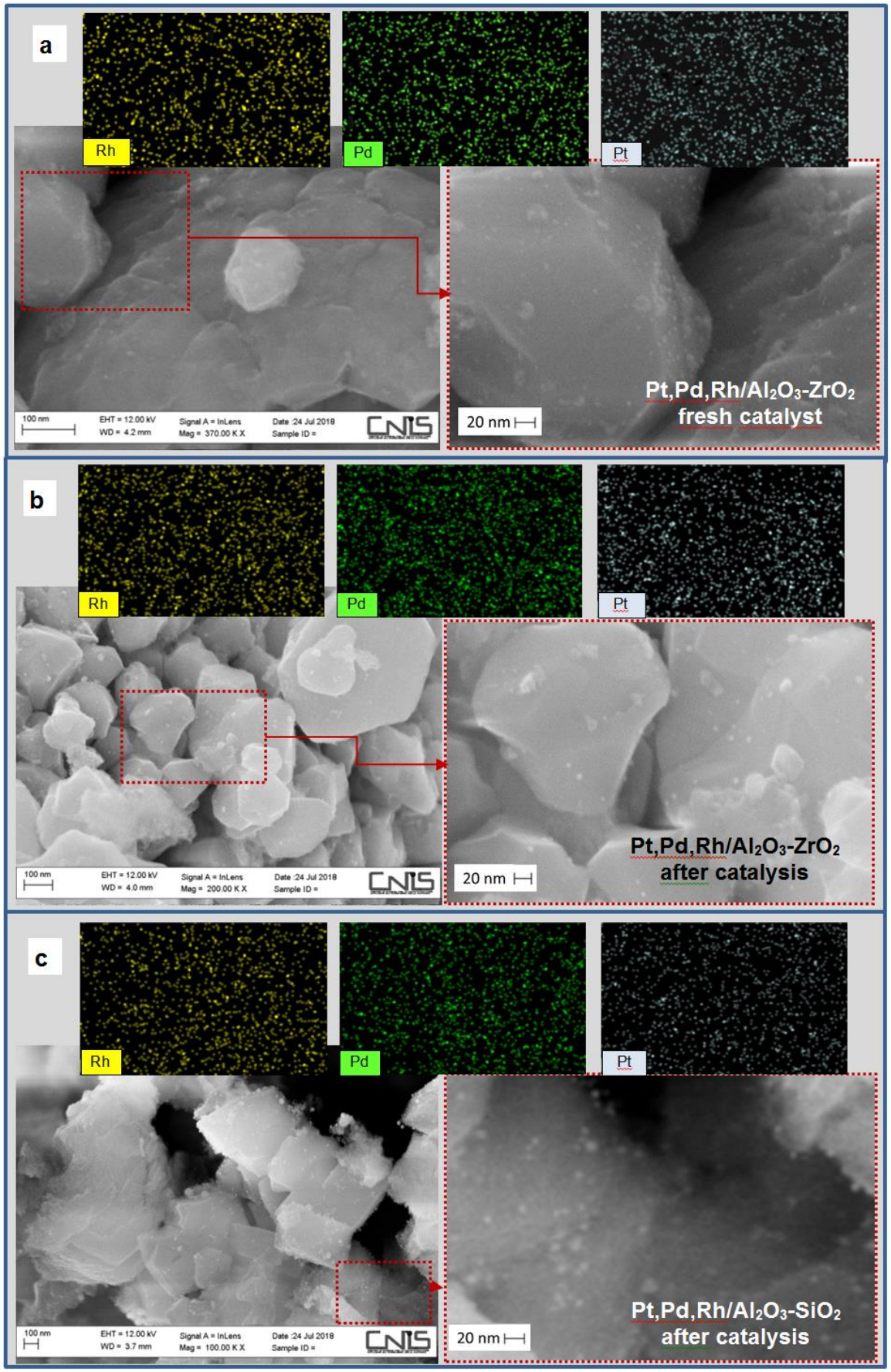

Figure 3. FESEM images of (a) fresh Pt,Pd,Rh/Al_2O_3-ZrO_2, (b) Pt,Pd,Rh/Al_2O_3-ZrO_2 after catalysis and (c) Pt,Pd,Rh/Al_2O_3-SiO_2 after catalysis. The insets are reporting the EDX elemental maps for the noble metals.

3.2. Catalytic activity

3.2.1. Simultaneous abatement of NO and N_2O with CH_4 in the presence or in the absence of O_2

With regard to the simultaneous abatement of NO and N_2O with CH_4 in the presence of O_2 (SCR_{sim}) the activity, as well as the selectivity to CO_2, of both Pt,Pd,Rh/Al_2O_3-SiO_2 and Pt,Pd,Rh/Al_2O_3-ZrO_2 catalysts were markedly depending on the oxygen content in the mixture. The behaviour at 500 °C for the Pt,Pd,Rh/Al_2O_3-SiO_2 catalyst is shown in Fig. 4a as a representative sample.

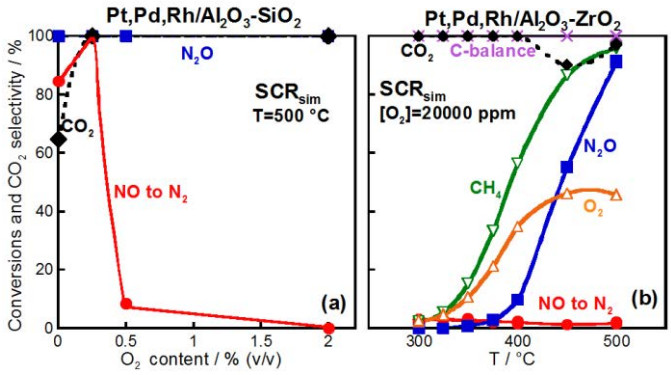

Figure 4. SCR_{sim} reaction. Section a: NO to N_2 (●), N_2O (■) conversions and CO_2 selectivity (◆) as a function of O_2 content in the mixture. Section b: NO to N_2 (●), N_2O (■), CH_4 (▽), O_2 (△) conversions, CO_2 selectivity (◆) and C-balance (✕) as a function of temperature. Reactant mixtures: $[N_2O]=[NO]=[CH_4]=4000$ ppm, $[O_2]=0\div20000$ ppm (total flow rate=50 cm^3 STP/min, He as balance). Catalysts as indicated.

For both catalysts, the SCR_{sim} was not effective over the entire range of temperature explored (250-500 °C) when O_2 was in large excess (20000 ppm), because the abatement of NO did not occur although N_2O was completely reduced above 375 °C (see Fig. 4b for Pt,Pd,Rh/Al_2O_3-ZrO_2). Almost the same catalytic behaviour was still observed for both catalysts when the amount of O_2 was decreased from 20000 to 5000 ppm (Figs. 5a and b). The SCR_{sim} became effective only by lowering further the O_2 content to 2500 ppm. In such conditions, the NO conversion to N_2 occurred and sharply increased with temperature, becoming complete above 400 °C (Figs. 5c and d). This behaviour is in agreement with the observed trend of NO conversion on similar Rh/ZrO_2 [35] and Ce–Zr promoted Pd–Rh/Al_2O_3 catalysts [32] in which the NO conversion decreased monotonically with increasing the air to fuel ratio (A/F) values. Our results showed that at the lowest O_2 amount explored by us (2500 ppm) N_2O conversion, slightly higher than that of NO, was promoted if compared to the

reaction at higher O_2 content (see Fig. 5). It should be noted that in the presence of O_2, the CO_2 selectivity was always 100% over the entire temperature range (Figs. 5 a-d). On the other hand, for the simultaneous NO and N_2O abatement in the absence of O_2 (CR_{sim}) both catalysts were slightly more effective than in SCR_{sim} reaction, as the NO and N_2O conversions were complete in the range 300-400 °C (Figs. 5e and f). However, the selectivity is worsening because the selectivity to N_2 and CO_2 were lower than in SCR_{sim}. In particular, due to CO formation, the CO_2 selectivity decreased to 60% as the temperature increased to 500 °C. Above 350 °C, the values of C and N mass balances were slightly less than 100% indicating the formation of small amounts of C- and/or N-containing by-products (like NH_3).

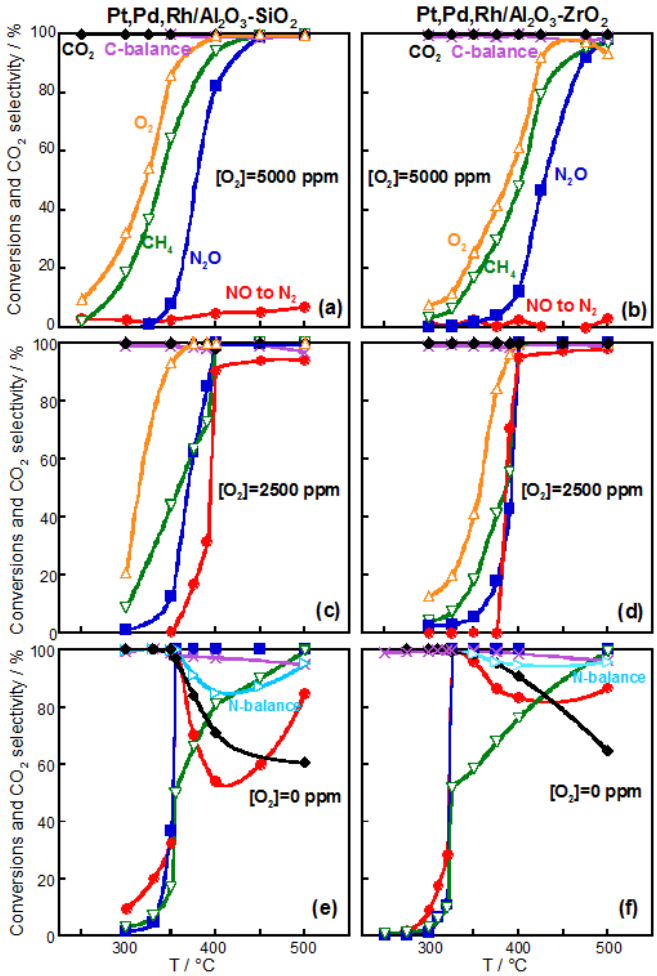

Figure 5. SCR_{sim} reaction on $Pt,Pd,Rh/Al_2O_3$-SiO_2 (Section a, c, e) and $Pt,Pd,Rh/Al_2O_3$-ZrO_2 (Section b, d, f) using $NO+N_2O+CH_4+O_2$ gas mixtures with different O_2 amount in the feed, as indicated. NO to N_2 (●), N_2O (■), CH_4 (▽), O_2 (△) conversions, CO_2 selectivity (◆), C-balance (✕) and N-balance (▷) as a function of temperature. Reactant mixtures: $[N_2O]=[NO]=[CH_4]=4000$ ppm, $[O_2]=0$, 2500 or 5000 ppm (total flow rate=50 cm^3 STP/min, He as balance).

With regard to CH_4 reactivity in SCR_{sim}, it should be noted that for all the values of O_2 concentration explored, i.e. 20000, 5000 and 2500 ppm, the CH_4 conversion on both catalysts was beginning at about 250 °C together with that of O_2, well before the range of temperatures at which the N_2O and NO started to be converted (about 325-375 °C, see Figs. 4b and 5a-d). This suggests that from 250 °C up to 325-375 °C only the competitive CH_4 combustion occurred. It should be also noted that at the lowest amount of O_2 (2500 ppm) and at higher temperatures, O_2 was almost completely consumed and CH_4 was fully converted as it reduced very effectively NO and N_2O (Figs. 5 c and d). This was confirmed by the CR_{sim}, in which the CH_4 conversion on both catalysts started at about 300 °C together with that of N_2O and NO (Figs. 5e and f). However, in the case of SCR_{sim} at 2500 ppm, the amount of O_2 in the mixture at higher temperatures, in spite of being very low, is enough to guarantee the 100% selectivity to CO_2 and N_2, thus avoiding the formation of the undesired by-products (Figs. 5c and d).

As a whole, these findings suggest that the activity and selectivity for SCR_{sim} strongly depend on the O_2/CH_4 feed ratio. With a feed mixture with O_2/CH_4 less than 1 (O_2/CH_4 = 2500/4000 v/v), O_2 was nearly completely consumed above 400 °C and the residual methane efficiently and simultaneously reduced NO and N_2O with negligible formation of by-products.

3.2.2. SCR_{N_2O}, SCR_{NO}, CR_{N_2O}, CR_{NO} and related reactions

In order to have more insight into the catalytic behaviour of both Pt,Pd,Rh/Al_2O_3-SiO_2 and Pt,Pd,Rh/Al_2O_3-ZrO_2 for the SCR_{sim} reaction, we measured the activity of catalysts for the CH_4+O_2 reaction (CH_4 combustion) which is the main competitive side-reaction affecting the selectivity during the NO and N_2O abatement by SCR. Moreover, for the same purpose, the separate NO and N_2O abatement reactions, either in the presence or in the absence of O_2 (i.e. SCR_{NO}, SCR_{N2O}, CR_{NO}, CR_{N2O}) were also investigated. The N_2O decomposition, by itself or in the presence of O_2 or NO, was also tested as probe reaction.

The activity of both catalysts for the CH_4 combustion was measured either with the lowest O_2 content (2500 ppm), at which the best performance for SCR_{sim} in terms of activity and selectivity was observed, or in the case of O_2 in large excess (20000 ppm). Irrespective of O_2 content, the light-off temperature of the CH_4+O_2 reaction was around 250 °C and CH_4 conversion increased with increasing temperature, becoming higher than 95% at 500 °C. These findings, as a whole, support the evidence that in the SCR_{sim} only the competitive CH_4 combustion occurred in the lower temperature range (from 250 °C up to 325-375 °C) at which N_2O and NO were unconverted. With regard to the CH_4 combustion, in agreement with literature [12,13], also in our case Pt and Pd are expected to be responsible for this reaction

acting possibly in a synergism. In particular, Pd is considered to be one of the most active for total oxidation of methane [36] and its activity, as metal or in oxidised state, increases with the increase of the oxygen vacancies on the PdO surface [37]. Based on these literature findings, in our conditions, although we observed only Pt metal after catalysis, it is reasonable that both Pd and Pt metals can be formed by reduction with CH_4 and that they can be re-oxidised along the reaction. Since in our catalysts the CH_4 combustion light-off temperature (ca. 250 °C) is almost the same either in defect or in the excess of O_2, we suggest that under the reaction condition the amount of the oxygen vacancies on the surface of Pd and Pt oxidised particles is independent of the amount of O_2 in the feed. As a whole these data suggest that the surface oxidation by O_2 is not limiting the reaction and that the CH_4 activation is very likely the relevant step in the oxidation reaction pathway.

The study of NO abatement in the reactions without N_2O (SCR_{NO} and CR_{NO}) showed that Pt,Pd,Rh/Al_2O_3-SiO_2 and Pt,Pd,Rh/Al_2O_3-ZrO_2 catalysts were both active for NO reduction by CH_4 with a similar activity. The inhibiting effect of O_2 on the NO conversion, already observed in the SCR_{sim}, is confirmed in the SCR_{NO} (Fig. 6a is reporting the data for Pt,Pd,Rh/Al_2O_3-SiO_2 as a representative case). In fact, whereas in the absence of O_2, i.e. CR_{NO}, NO is completely converted to N_2 in a very short range of temperature close to 300 °C, in the presence of O_2, i.e. SCR_{NO}, NO conversion was remarkably inhibited, starting at about 350 °C with 2500 ppm and at 400 °C with 5000 ppm of O_2 (Fig. 6a). The observed inhibiting effect of O_2 on the NO conversion could be explained by taking into account that, as in SCR_{sim}, also in SCR_{NO} the CH_4 combustion occurred preferentially instead of NO reduction in the lower temperature range, as confirmed by the parallel starting of CH_4 and O_2 consumption in the lower temperature range (Figs. 7c and d). The high activity for CH_4 combustion has been ascribed to the Pd/PdO species in the catalysts also in the presence of NO [38]. On the other hand, in the absence of O_2 (CR_{NO}) or in SCR_{NO} at high temperature when O_2 is almost completely consumed, CH_4 could reduce the noble-metal ions to metal state on the catalyst surface, as it was found in a NO+C_xH_y reaction where the reduction of transition metal ions can occur by hydrocarbon [39,40,41]. According to literature [8], on a reduced noble metal surface the dissociation of NO can occur, giving $N_{(ads)}$ and $O_{(ads)}$, with subsequent desorption of N_2 and removal of $O_{(ads)}$ by the reductant (CH_4 in our case). In the case of the three-way Rh-Pd-Pt-containing catalysts, the Rh metal plays a relevant role for the NO dissociation [10,42] and for NO reduction because it can be oxidized more easily than Pd and Pt noble metals [3]. These literature considerations may explain why in our case, in the SCR_{NO} reaction, NO was unconverted in the lower temperature range at which O_2 was still present

thus preserving the noble metals in the oxidized state. In the lower temperature range, Pt and Pd, that are considered to promote the oxidation reaction [37,42], activate CH_4 for the competitive combustion.

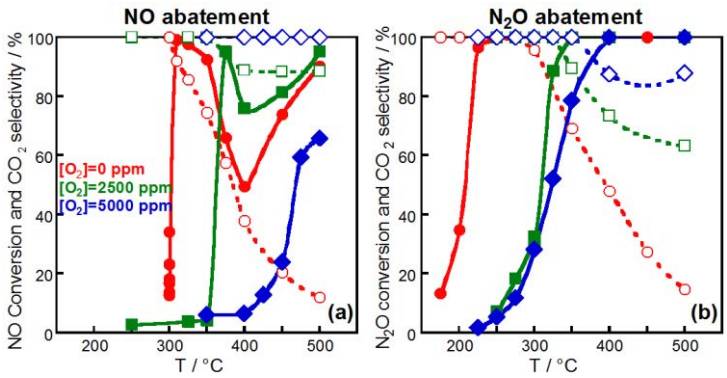

Figure 6. Effect of O_2 on the NO and N_2O abatement with CH_4 using gas mixtures with different O_2 amount in the feed, as indicated. Section a: NO conversion to N_2 (closed symbols) and CO_2 selectivity (open symbols) for the CR_{NO} and SCR_{NO} reactions as a function of temperature. Section b: N_2O conversion (closed symbols) and CO_2 selectivity (open symbols) for the CR_{N2O} and SCR_{N2O} reactions as a function of temperature. Catalyst: Pt,Pd,Rh/Al_2O_3-SiO_2. Reactant mixtures: [NO] or [N_2O]=[CH_4]=4000 ppm, [O_2]= 0 (●,○), 2500 (■,□) or 5000 ppm (◆,◇), (total flow rate=50 cm^3 STP/min, He balance).

In the case of CR_{NO}, it should be noted that on both catalysts, while the NO conversion was complete above 300 °C, the NO conversion to N_2 remarkably decreased from 300 to 400 °C, and then increased again above 400 °C although never reaching 100% (Fig. 7a and b). This behaviour is a solid piece of evidence that the formation of some N-containing by-products (likely NH_3, as N_2O was never detected), occurred. Moreover, such N-containing by-products are not containing C species, as the C-balance was nearly 100% in the whole temperature range explored. With regard to the CO_2 selectivity, it markedly decreased as temperature increased, becoming less than 20% at 500 °C. In the SCR_{NO}, the presence of O_2 improved the selectivity to N_2 and CO_2. In particular, at the lowest content of O_2 (2500 ppm), the CO_2 selectivity was at least 80% at 500 °C, and a lower amount of N-containing by-products were formed (Figs. 7c and d).

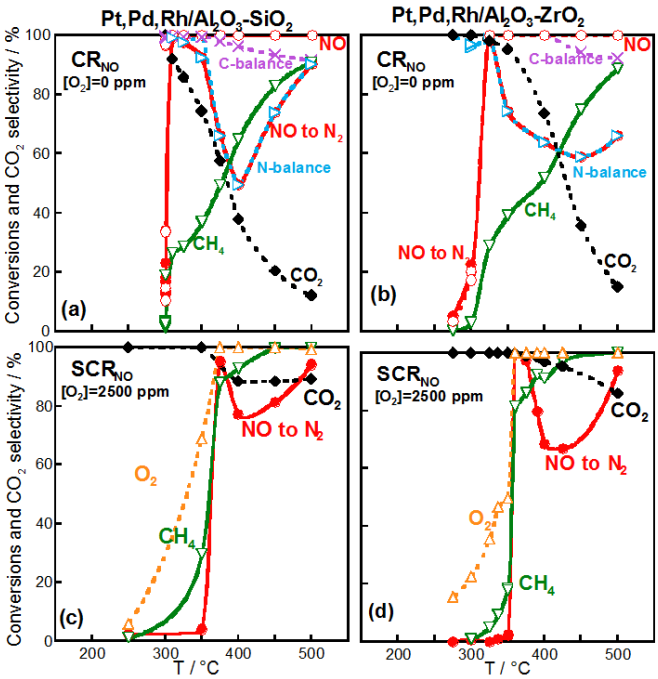

Figure 7. CR_{NO} and SCR_{NO} reactions on Pt,Pd,Rh/Al_2O_3-SiO_2 (Section a and c, respectively) and Pt,Pd,Rh/Al_2O_3-ZrO_2 (Section b and d, respectively). NO to N_2 (●), CH_4 (▽), O_2 (△) conversions, CO_2 selectivity (◆), C-balance (✕) and N-balance (▷) as a function of temperature. In the absence of O_2, also total NO conversion (○) was calculated. Reactant mixtures: [NO]=[CH_4]=4000 ppm, [O_2]=0 or 2500 ppm (total flow rate=50 cm^3 STP/min, He as balance).

The study of N_2O abatement in the reactions without NO (SCR_{N2O} and CR_{N2O}) showed that Pt,Pd,Rh/Al_2O_3-SiO_2 and Pt,Pd,Rh/Al_2O_3-ZrO_2 catalysts were both active for N_2O reduction by CH_4. If, on the one hand, the presence of O_2, regardless of its amount (2500 or 5000 ppm), negatively affected the N_2O conversion, as clearly evidenced by the shift of its light-off temperature to higher values, on the other hand O_2 in the feed remarkably increased the CO_2 selectivity (Fig. 6b). In the absence of O_2, i.e. CR_{N2O}, the N_2O conversion is starting at rather low temperature (about 150 °C for Pt,Pd,Rh/Al_2O_3-SiO_2 and about 100 °C for Pt,Pd,Rh/Al_2O_3-ZrO_2) and was almost complete at about 225 °C (Figs. 8a and b). In this range of temperature and up to 300 °C, the CH_4 conversion followed the $CH_4+4N_2O \rightarrow 4N_2+CO_2+2H_2O$ stoichiometry, as confirmed by the CO_2 selectivity which was 100%. Above 300 °C, the reaction $CH_4+N_2O \rightarrow N_2+CO+2H_2$ is gradually prevailing, as suggested by the remarkable increase of CH_4 conversion and the strong decrease of CO_2 selectivity to CO. Moreover, the C-balance decreased to about 90% at 500 °C, while the N-balance was always 100%, this being coherent with the formation of a small amount of undefined $C_xH_yO_z$ by-products.

In SCR_{N2O} (Figs. 8c and d), the N_2O and CH_4 conversions started at nearly the same temperature and, on increasing temperature, they are overlapping. This behaviour suggests the occurrence of $CH_4+N_2O+3/2O_2 \rightarrow N_2+CO_2+2H_2O$ stoichiometry and excludes the combustion as a side-reaction in a narrow range of temperature (250-325 °C). Above 325 °C, O_2 was completely consumed and the reaction followed a stoichiometry resembling that occurring for the CR_{N2O}. It is interesting to note that differently from CR_{N2O}, in the SCR_{N2O} the N_2O conversion is starting at higher temperature for the Pt,Pd,Rh/Al_2O_3-ZrO_2 catalyst if compared to the Pt,Pd,Rh/Al_2O_3-SiO_2 catalyst (275°C vs. 225°C, Fig. 8).

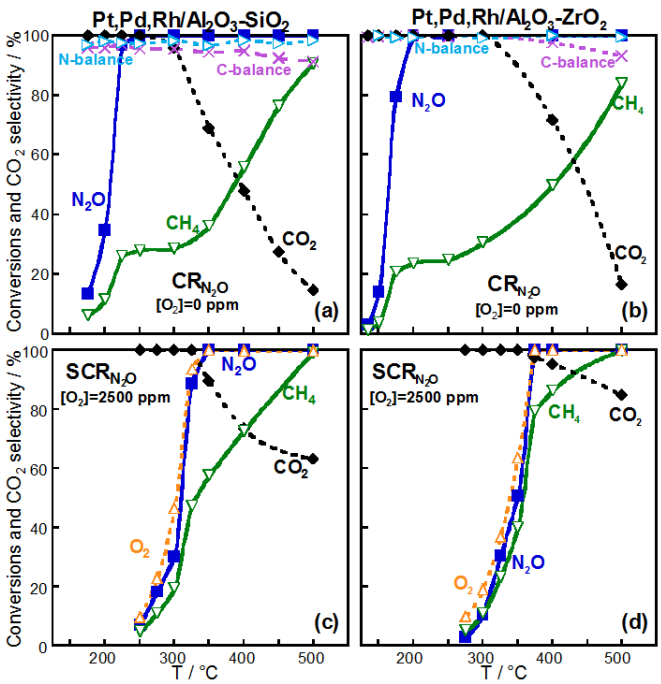

Figure 8. CR_{N2O} and SCR_{N2O} reactions on Pt,Pd,Rh/Al_2O_3-SiO_2 (Section a and c, respectively) and Pt,Pd,Rh/Al_2O_3-ZrO_2 (Section b and d, respectively). N_2O (■), CH_4 (▽), O_2 (△) conversions, CO_2 selectivity (◆), C-balance (✕) and N-balance (▷) as a function of temperature. Reactant mixtures: $[N_2O]=[CH_4]=4000$ ppm, $[O_2]=0$ or 2500 ppm (total flow rate=50 cm^3 STP/min, He as balance).

As our results showed that O_2 affects the NO and N_2O conversion, suggesting that the mobility of the adsorbed oxygen species, regardless of their origin (coming from N_2O, or NO or O_2) are playing a relevant role in sustaining the conversion of NO and N_2O, a study of the N_2O decomposition as a probe reaction was made. We chose this reaction because it is well known that gaseous N_2O adsorbs on cationic active sites through O-end, yielding decomposition into N_2 and O_{ads} species, according to the following generalized redox mechanism [43]) on the surface active site *:

$N_2O + * \rightarrow N_2O*$ (1)

$N_2O* \rightarrow N_2 + O*$ (2)

$2O* \rightarrow O_2 + 2*$ (3)

The pairing of O_{ads} species to form gaseous O_2 (step 3) is generally considered as the rate-limiting step and it is strongly dependent on the O_{ads} mobility on the surface and on the strength of the O-site bonding. In our case, on both Pt,Pd,Rh/Al_2O_3-SiO_2 and Pt,Pd,Rh/Al_2O_3-ZrO_2 catalysts the N_2O conversion was characterized by a very steep growth leading the conversion to reach 100% value in a very short range of temperature close to 300 °C (Fig. 9a). Such a very steep growth looks like a threshold temperature at which the surface mobility of the adsorbed oxygen species seems to become high enough to give an easy O_2 desorption, thus making free the sites for the N_2O adsorption that can quickly decompose. The difficulty related to the mobility of adsorbed oxygen species and the consequent desorption of molecular O_2 is overcome when CH_4 is added to the feed, because it removes the adsorbed-O species thus decreasing remarkably the light-off temperature to 150 °C (see Fig. 8a and b). This is in agreement with recent literature data showing that, on alumina supported Pd catalysts, the N_2O decomposition activity is remarkably increased when C_3H_6 was added as a reductant lowering the temperature required for 100% conversion [44]. The promotional effect of CH_4 can occurs in two ways: (i) by removing O ad-atoms from the noble metals, thereby maintaining them in a more reduced state; (ii) by removing O from the Al_2O_3-ZrO_2 or Al_2O_3-SiO_2 supports surface thereby creating O vacancies. In absence of CeO_2 in our supports which is known to store and release oxygen in the CeO_2-ZrO_2 based catalysts [12,42], it is more likely that the removal of O-species is from the noble metals.

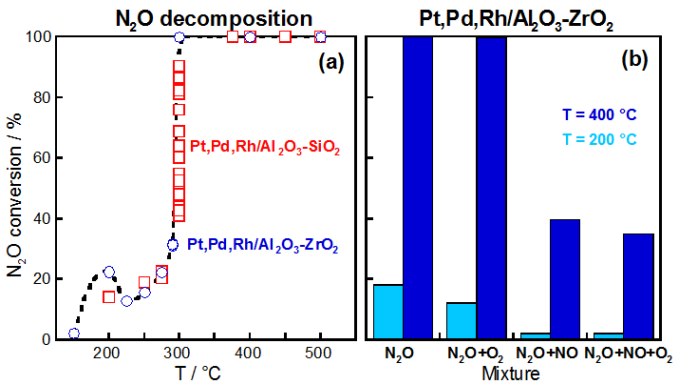

Figure 9. N_2O abatement on Pt,Pd,Rh/Al_2O_3-SiO_2 (□) and Pt,Pd,Rh/Al_2O_3-ZrO_2 (○) catalysts. Section a: N_2O conversion in N_2O decomposition as a function of temperature. Section b: N_2O conversion at 200 or 400 °C for N_2O decomposition, or after addition to the N_2O feed of O_2 and NO, separately or together (as specified). Reactant mixtures: [N_2O]=4000 ppm, [NO]=0 or 4000 ppm, [O_2]=0 or 2500 ppm (total flow rate=50 cm^3 STP/min, He as balance).

Some further valuable details on the abatement reactions were provided by the experiment in which O_2 and NO separately , or O_2+NO were added to N_2O feed (Fig. 9b).

The addition of O_2 to the N_2O feed did not change the N_2O decomposition catalytic activity above the threshold-like temperature (300 °C), whereas at lower temperature a slight decrease of N_2O conversion was observed. The absence of reaction inhibition by O_2 at high temperatures (in our case, above 300 °C) has been explained in the literature suggesting that O_2 does not compete with the N_2O adsorption sites [43,45], and therefore O_2 does not contribute to the overall surface O-coverage. At low temperatures (in our case, below 300 °C), a competitive adsorption between O_2 and N_2O may occur as the surface mobility of the adsorbed oxygen species is lower.

On the other hand, the addition of NO to the N_2O feed negatively affected the N_2O decomposition, which was remarkably depressed as evidenced by the shifting of the light-off temperature of about 100 °C to higher values. These results suggest that, differently from O_2, the active sites for the N_2O decomposition are poisoned by the addition of NO that, upon adsorption and reaction with O-species released upon N_2O adsorption, likely formed some NO_y-like (nitrites/nitrates) species strongly adsorbed on the same sites active for the N_2O decomposition. Interestingly, the addition of O_2 to the N_2O+NO mixture, did not further affect the N_2O conversion which, however, remarkably increased when CH_4 was added to the mixture (i.e. SCR_{sim}). Such behaviour may be explained by suggesting that CH_4 made again free the active sites likely reacting with the suggested adsorbed NOy-like species or by consuming O adsorbed species (coming from either O_2 or N_2O).

According to the ability of N_2O to adsorb dissociatively on metal ions, as in CR_{N2O}, even in the SCR_{N2O} the oxygen species reacting with CH_4 are likely those mainly coming from N_2O which left a reactive oxygen on the surface. This conclusion is supported by the evidence that the stoichiometry of the SCR_{N2O} reaction remained unchanged on changing the amount of O_2, with no other side-reactions, in particular the CH_4 combustion. The increase of the amount of O_2 in the feed mixture was beneficial for the CO_2 selectivity which increased although it never reached 100%. This finding can be explained by taking into account that, at higher temperatures where high N_2O and CH_4 conversions occurred, the O_2 amount was slightly lower than the stoichiometric value either at 2500 or 5000 ppm, thus leading to the formation of a small amount of CO.

As a whole, these results suggest that in the temperature region below the threshold-like temperature (about 300 °C) where the mobility of surface O-species is low, the CH_4 easily reacted with the surface O-species released by N_2O, thus guaranteeing a high CR_{N2O} activity

even at lower temperatures. By adding O_2, the competitive adsorption between N_2O and O_2 caused the decrease of the amount of such reactive adsorbed-O species, thus shifting the light-off of the SCR_{N2O} to higher temperatures where the mobility of adsorbed-O species was remarkably increased and the competitive adsorption was largely decreased.

From Fig.8 it appears that Pt,Pd,Rh/Al_2O_3-ZrO_2 catalyst has superior activity in CR_{N2O} but inferior activity in SCR_{N2O} in comparison with the Pt,Pd,Rh/Al_2O_3-SiO_2 catalyst. Although on a speculative basis, an attempt to explain such a difference may be made if the role of the support is taken into account. In the Pt,Pd,Rh/Al_2O_3-ZrO_2 catalyst, the ZrO_2 may play a role in improving noble metals dispersion and redox ability on the catalyst surface, as reported for Rh in Rh/Ce-ZrO_2 catalyst for the N_2O decomposition [46]. Moreover, a beneficial effect of ZrO_2 for the same reaction has been also reported in the case of Ir/ZrO_2 catalyst which exhibited particularly high performance if compared to Ir on other supports, in particular with respect to SiO_2 that resulted to be the worst [47]. These findings can be extended to Rh, recalling that Rh and Ir have a similar activity on supported catalysts for the N_2O decomposition [14]. The considerations above can support the idea that the presence of ZrO_2, differently from SiO_2, can possibly enhance the reactivity of N_2O making easier the N_2O activation step on the Pt,Pd,Rh/Al_2O_3-ZrO_2 catalyst in the CR_{N2O} reaction.

On the other hand, when O_2 is added to N_2O+CH_4 feed, i.e. in the case of SCR_{N2O}, since O_2 can adsorb competitively with N_2O on the same sites (vide supra), the improved noble metals dispersion and redox ability could make more competitive the adsorption of O_2 with respect to N_2O, thus leading to a lower activity of the Pt,Pd,Rh/Al_2O_3-ZrO_2 catalyst with respect to Pt,Pd,Rh/Al_2O_3-SiO_2 catalyst for SCR_{N2O} below 300 °C.

3.2.3. Comparison of SCR_{sim} with the related reactions

A comparison of SCR_{sim} at 2500 ppm of O_2 with the homologous separate abatement reactions, i.e. SCR_{N2O} and SCR_{NO} (see Figs. 10a and b) provides some further information on the investigated reactions. For both the Pt,Pd,Rh/Al_2O_3-SiO_2 and Pt,Pd,Rh/Al_2O_3-ZrO_2 catalysts, the presence of NO has a detrimental effect on the N_2O abatement. In fact if we look at the SCR_{sim}, the N_2O conversion is starting at much higher temperature (about 300 °C) with respect to that observed when N_2O is alone (about 225 °C), i.e. in SCR_{N2O}, suggesting that adsorbed NO species, including its derivative (NOy-like species), likely poisoned the active sites for the N_2O activation. This is confirmed by comparing the N_2O decomposition probe reaction with the reaction in which NO was added to the N_2O feed, leading to a detrimental effect on the N_2O conversion (Fig. 9b). As a whole, these results support the hypothesis that

the poisoning species for the N_2O adsorption active sites are some NOy-like species formed from the reaction of NO with the surface O-species.

On the other hand, on both catalysts the presence of N_2O has a much lower impact on the NO abatement activity (see Figs. 10a and b), as the NO conversion is starting only at slightly higher temperature of about 25 °C with respect to that observed in SCR_{NO}, which suggests that a small competitive effect due to the N_2O adsorption on the same sites active for NO reduction was occurring. However, the presence of N_2O has a beneficial effect on the NO abatement selectivity, as shown by the fact that NO converted to N_2 alone in SCR_{sim}, whereas large amounts of N-containing by-products were formed in the SCR_{NO}.

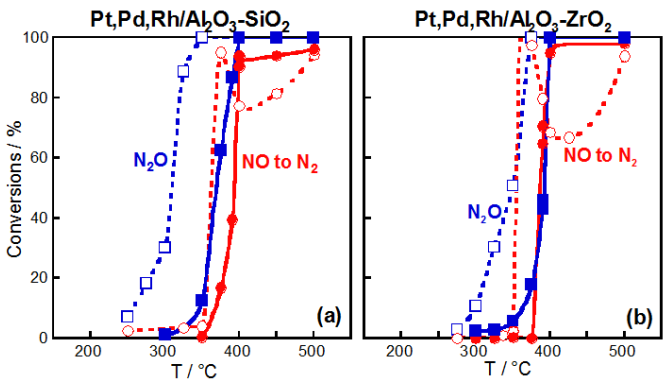

Figure 10. Comparison between SCR_{sim} and the related SCR_{NO} and SCR_{N2O} reactions on Pt,Pd,Rh/Al_2O_3-SiO_2 (Section a) and Pt,Pd,Rh/Al_2O_3-ZrO_2 (Section b). NO to N_2 (○,●) and N_2O (□,■) conversions as a function of temperature. Open symbols: SCR_{NO} ([NO]=[CH_4]=4000 ppm, [O_2]=2500 ppm) and SCR_{N2O} ([N_2O]=[CH_4]=4000 ppm, [O_2]=2500 ppm). Closed symbols: SCR_{sim} ([N_2O]=[NO]=[CH_4]=4000 ppm, [O_2]=2500 ppm).

The same reciprocal effect of the addition of NO to N_2O, and the reverse, was observed also in the absence of O_2 (i.e. CRsim, CR_{NO}, CR_{N2O}). Indeed on both catalysts N_2O reduction in CR_{N2O} was remarkably hampered by adding NO to the feed, causing the light-off to shift about 150 °C to higher temperature, whereas NO reduction in CR_{NO} was only slightly affected by adding N_2O to the feed.

The comparison of CH_4 conversion with O_2, or NO, or N_2O on the Pt,Pd,Rh/Al_2O_3-ZrO_2 catalyst, that gives an insight into the active site reactivity, is reported in Fig. 11.

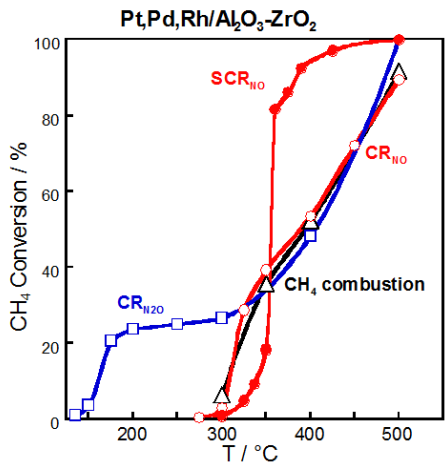

Figure 11. CH_4 reactivity with (i) O_2 (CH_4 combustion, △), (ii) N_2O (CR_{N2O}, □), (iii) NO (CR_{NO}, ○) and (iv) $NO+O_2$ (SCR_{NO}, ●). CH_4 conversion as a function of temperature on $Pt,Pd,Rh/Al_2O_3$-ZrO_2. Reactant content in the mixtures: $[N_2O]=[NO]=[CH_4]=4000$ ppm, $[O_2]= 2500$ ppm (total flow rate=50 cm^3 STP/min, He as balance).

It is clearly evident that CH_4 much more easily reacted with N_2O, the conversion starting at lower temperature (150 °C) if compared to the reactions with O_2 or NO (300 °C). Interestingly, the reactivity of CH_4 with O_2 or NO is almost the same, as shown by the corresponding conversion curves that are almost overlapping. It should be noted that this reactivity started at the threshold-like temperature (about 300 °C) at which the high mobility of the surface oxygen species is enhancing the reactant activation. This suggests that in both CR_{NO} and CH_4 combustion CH_4 is very likely activated on the catalyst surface thus reacting with NO or O_2 in the gas phase. On the other hand, the temperature at which the CH_4+N_2O reaction started is much lower than that of the CH_4 combustion but almost the same as which the N_2O decomposition started (about 150 °C, see Fig. 9a). This finding suggests that at this temperature (150 °C) the O-species released along the N_2O adsorption became reactive with CH_4. While the reactivity of CH_4 with O_2 or NO separately is almost the same, it was depressed in the lower temperature range when the two reactants $NO+O_2$ were present in the feed (Fig. 11). Keeping in mind that at lower temperatures CH_4 conversion during SCR_{NO} is due only to the combustion, this result supports the idea that the adsorbed NO_y-like species formed in the presence of O_2 are poisoning also the active sites for the CH_4 combustion.

4. Conclusions

$Pt,Pd,Rh/Al_2O_3$-SiO_2 and $Pt,Pd,Rh/Al_2O_3$-ZrO_2 are promising catalysts for the simultaneous abatement of NO and N_2O in the SCR with CH_4 from feeds containing O_2/CH_4 less than 1, yielding complete NO and N_2O conversions above 400 °C. In such conditions, i.e.

low O_2 amount, (i) a partial reduction of the noble metal ions by CH_4 may guarantee the N_2O and NO activation and (ii) the simultaneous presence of NO and N_2O in the stream guarantees the complete selectivity to CO_2 and N_2. However, a slight shift of activity towards higher temperatures occurs if compared to the separate NO and N_2O abatement reactions. This shift is suggested to be related to the possible formation of some strongly adsorbed NO_y-like species formed along NO adsorption on the catalyst and competing with the N_2O adsorption active sites. The poisoning effect of the NO_y-like adsorbed species is confirmed in the SCR_{NO} and in the N_2O abatement in the presence of NO or NO+O_2. This poisoning effect disappears above a threshold-like temperature (about 300 °C), but only if O_2 is not in a large amount. At this temperature the surface-O mobility is high enough to sustain the reduction of both NO and N_2O.

In such complex reactions a role of the support cannot be excluded. If compared to the Pt,Pd,Rh/Al_2O_3-SiO_2 material, in the Pt,Pd,Rh/Al_2O_3-ZrO_2 catalyst the ZrO_2 may play a role in improving noble metals dispersion and their redox ability on the catalyst surface, these properties affecting in some cases the catalytic behavior. On the other hand, in spite of the rather different noble metals content, the Pt,Pd,Rh/Al_2O_3-SiO_2 and Pt,Pd,Rh/Al_2O_3-ZrO_2 catalysts do not show a remarkably different catalytic behaviour for the SCR_{sim}. Since the FESEM analysis suggests a rather homogeneous dispersion of the noble metals on both supports, it can be reasonably inferred that, at least for this reaction, only a fraction of the total amount of noble metals, likely those exposed on the surface of particles in a peculiar contact with the support, is playing the role of the active site in the SCR_{sim} . This makes this system attractive from a practical point of view, as a rather low content of highly expensive noble metals is effective to have a high activity.

Acknowledgments

We gratefully acknowledge “Sapienza” University of Rome for financial support (Research Project 2016 - Grant n. RG116154E1F7B680).

References

[1] A.R. Ravishankara, J.S. Daniel, R.W. Portmann, Science 326 (2009) 123-125.

[2] M. Piumetti, S. Bensaid, D. Fino, N. Russo, Catal. Struct. React. 1 (2015) 155-173.

[3] P. Bera, M.S. Hedge, Catal. Surv. Asia 15 (2011) 181-199.

[4] P. Forzatti, L. Lietti, E. Tronconi, Nitrogen oxides removal industrial in Encyclopedia of Catalysis, Wiley Online Library, 2010, https://doi.org/10.1002/0471227617.eoc155.pub2

[5] B. Guan, R. Zhan, H. Lin, Z. Huang, Appl. Therm. Eng. 66 (2014) 395-414.

[6] W. Shan, H. Song, Catal. Sci. Technol. 5 (2015) 4280-4288.

[7] R. Marques, L. Mazri, S. Da Costa, F. Delacroix, G. Djéga-Mariadassou, P. Da Costa, Catal. Today 137 (2008) 185-190.

[8] R. Burch, J.P. Breen, F.C. Meunier, Appl. Catal. B 39 (2002) 283–303.

[9] C. Huang, W. Shan, Z. Lian, Y. Zhang, H. He, Catal. Sci. Technol. 10 (2020) 6407-6419. https://doi.org/10.1039/D0CY01320J

[10] P. Granger, V.I. Parvulescu, Chem. Rev. 111 (2011) 3155–3207.

[11] J. Song, M. Choi, J. Lee, J.M. Kim, Int. J. Automotive Tech. 21 (2020) 441–449.

[12] S. Rood, S. Eslava, A. Manigrasso, C. Bannister, Proc IMechE Part D: J. Automobile Engineering 234 (2020) 936–949.

[13] Y. Jung, Y.D. Pyo, J. Jang, G.C. Kim, C.P. Cho, C. Yang, Chem. Eng. J. 369 (2019) 1059–1067.

[14] M. Konsolakis, ACS Catal. 5 (2015) 6397–6421.

[15] M. Jabłońska, R. Palkovits, Catal. Sci. Technol. 6 (2016) 7671-7687.

[16] R.W. van den Brink, S. Booneveld, M.J.F.M. Verhaak, F.A.de Bruijn, Catal. Today 75 (2002) 227-232.

[17] G.E. Marnellos, E.A. Efthimiadis, I.A. Vasalos, Ind. Eng. Chem. Res. 43 (2004) 2413-2419.

[18] Y. Wu, C. Dujardin, C. Lancelot, J.P. Dacquin, V.I. Parvulescu, M. Cabié, C.R. Henry, T. Neisius, P. Granger, J. Catal. 328 (2015) 236–247

[19] F. Schuricht, W. Reschetilowski, Micropor. Mesopor. Mater. 164 (2012) 135-144.

[20] S.J. Lee, I.S. Ryu, S.G. Jeon, S.H. Moon, Environ. Prog. Sustain. 38 (2019) 451-456.

[21] J.H. Baek, S.M. Lee, J.H. Park, J.M. Jeong, R.H. Hwang, C.H. Ko, S.G. Jeon, T.H. Choi, K.B. Yi, J. Ind. Eng. Chem. 48 (2017) 194-201.

[22] A. Guzmán-Vargas, G. Delahay, B. Coq, Appl. Catal. B 42 (2003) 369-379.

[23] B. Coq, M. Mauvezin, G. Delahay, J.-B. Butet, S. Kieger, Appl. Catal. B 27 (2000) 193-198.

[24] J. Perez-Ramirez, F. Kapteijn, Catal. Commun. 4 (2003) 333-338.

[25] M. Kögel, R. Mönnig, W. Schwieger, A. Tissler, T. Tureka, J. Catal. 182 (1999) 470-478.

[26] Brochures of EnviNOx, are available at http://www.uhde.biz.

[27] G. Mul, J. Pérez-Ramírez, F. Kapteijn, J.A. Moulijn, Catal. Letters 77 (2001) 7-13.

[28] J. Pérez-Ramírez, F. Kapteijn, G. Mul, J.A. Moulijn, J. Catal. 208 (2002) 211-223.

[29] M.C. Campa, D. Pietrogiacomi, C. Scarfiello, L.R. Carbone, M. Occhiuzzi, Appl. Catal. B 240 (2019) 367-372.

[30] M.C. Campa, D. Pietrogiacomi, M. Occhiuzzi, Appl. Catal. B 168-169 (2015) 293-302.

[31] D. Pietrogiacomi, M.C. Campa, L. Ardemani, M. Occhiuzzi, Catal. Today 336 (2019) 131-138.

[32] D. Bounechada, G. Groppi, P. Forzatti, K. Kallinen,T. Kinnunen, Top. Catal. 56 (2013) 372–377.

[33] R.K. Biswas, P. Khan, S. Mukherjee, A.K. Mukhopadhyay, J. Ghosh, K. Muraleedharan, J. Non-Cryst. Solids 488 (2018) 1-9.

[34] P. Scherrer, Nachr. Ges. Wiss. Göttingen, 26 (1918) 98-100.

[35] H. Yoshida, R. Kakei, Y. Kuzuhara, S. Misumi, M. Machida, Catal. Today 332 (2019) 245-250.

[36] P. Gélin, M. Primet, Appl. Catal. B 39 (2002) 1–37.

[37] A.W. Petrov, D. Ferri, F. Krumeich, M. Nachtegaal, J.A. van Bokhoven, O. Kröcher, Nat. Commun. 9 (2018) 2545. https://doi.org/10.1038/s41467-018-04748-x

[38] Y. Lu, K.A. Michalow, S.K. Matam, A. Winkler, A.E. Maegli, S. Yoon, A. Heel, A. Weidenkaff, D. Ferri, Appl. Catal. B 144 (2014) 631– 643.

[39] G. Ferraris, G. Fierro, M. Lo Jacono, M. Inversi, R. Dragone, Appl. Catal. B 36 (2002) 251-260.

[40] G. Ferraris, G. Fierro, M. Lo Jacono, M. Inversi, R. Dragone, Appl. Catal. B 45 (2003) 91-101.

[41] G. Fierro, G. Ferraris, R. Dragone, M. Lo Jacono, M. Faticanti, Catal. Today 116 (2006) 38–49.

[42] J. Kašpar, P. Fornasiero, N. Hickey, Catal. Today 77 (2003) 419-449.

[43] F. Kapteijn, J. Rodriguez-Mirasol, J.A. Moulijn, Appl. Catal. B 9 (1996) 25-64.

[44] N. Richards, J.H. Carter, E. Nowicka, L.A. Parker, S. Pattisson, Q. He, N.F. Dummer, S. Golunski, G.J. Hutchings, Appl. Catal. B 264 (2020) 118501. https://doi.org/10.1016/j.apcatb.2019.118501

[45] D. Pietrogiacomi, M.C. Campa, L.R. Carbone, S. Tuti, M. Occhiuzzi, Appl. Catal. B 187 (2016) 218-227.

[46] M.-J. Kim, H.J. Kim, S.-J. Lee, I.-S. Ryu, H.C. Yoon, K.B. Lee, S.G. Jeon, Catal. Commun. 130 (2019) 105764. https://doi.org/10.1016/j.catcom.2019.105764

[47] S. Hinokuma, T. Iwasa, Y. Kon, T. Taketsugu, K. Sato, Catal. Commun. 149 (2021) 106208. https://doi.org/10.1016/j.catcom.2020.106208